DEVELOPMENT OF A PHOTOCATHODE RF GUN FOR AN L-BAND ELECTRON LINAC

S. Kashiwagi#, R. Kato, Y. Morio, K. Furuhashi, Y. Terasawa, N. Sugimoto, G. Isoyama,
ISIR, Osaka University, Ibaraki, Osaka, 567-0047, Japan
H. Hayano, H. Sugiyama, J. Urakawa, K. Watanabe,
KEK, Tsukuba, Ibaraki 305-0801, Japan
M. Kuriki, C. Shonaka and D. Kubo
AdSM, Hiroshima University, Higashi-Hiroshima, Hiroshima 739-8511, Japan

Abstract

We conduct research on Free Electron Laser (FEL) in the infrared region and pulse radiolysis for radiation chemistry using the 40 MeV, 1.3 GHz L-band linac of Osaka University. At present, the linac is equipped with a thermionic electron gun. It can accelerate a high-intensity single-bunch beam with charge up to 91 nC but the normalized emittance is large. In order to advance the research, we have begun development of a photocathode RF gun for the L-band linac in collaboration with KEK and Hiroshima University. A new design of the L-band RF gun cavity that improves the cooling system for a long RF pulse operation is being developed and the ultra-precision machining is given to the fabrication of the RF gun cavity. The simulation is also performed for the case of a high charge electron beam. Before we install the new L-band RF gun into the L-band linac of Osaka University, we plan to commission the DESY type of L-band RF gun at the Superconducting RF Test Facility of KEK (KEK-STF). The DESY type of gun is fabricated at the Fermi National Accelerator Laboratory (FNAL), and the resonant frequency and field balance of the RF gun cavity have been adjusted using a tuning apparatus at KEK-STF. In this conference, we describe details of the L-band RF gun development.

PHOTOCATHODE RF GUN FOR L-BAND ELECTRON LINAC AT ISIR, OSAKA UNIVERSITY

Conceptual Design

We start basic design of the RF gun for the L-band linac at ISIR, Osaka University, based on the 1.5 cells RF gun, which is a normal conducting photo-cathode RF gun used at many laboratories and therefore time-tested. The photo-cathode should be Cs_2Te, which has the high quantum efficiency of a few percents, to produce a beam with high charge up to 30 nC/bunch. One of the objectives of this study is to develop an RF gun meeting specifications required for the International Linear Collider (ILC) Project. The dark current due to the field emission, which is the cause of discharge, should be low and the heat produced on the cavity wall has to be efficiently removed and accordingly the deformation of the cavity shape due to the heat be suppressed for the input power of 5 MW with the pulse duration of 1 ms and the repetition rate of 5 Hz.

An extremely high accelerating field can be produced in the RF gun. With the increase of the electric field, however, the dark current produced on the cavity wall increases, resulting in the higher possibility of destructive discharge in the cavity, so that it is necessary to reduce the dark current to stably produce an electron beam. We plan to use oxygen-free copper of the class-1 treated by the hot isostatic pressing (HIP) process as materials of the RF cavity and to turn it off with an ultra-precision lathe and a diamond cutting-tool. After components being machined, they will be brazed without any cleaning processes like electrochemical polishing and the ozone wash [1, 2].

The other crucial issue is the heat load. The average input power of the RF gun is calculated to be 25 kW. The RF cavity is made of copper and its weight is estimated to be 47.5 kg. The temperature of the cavity will rise by 1.37 K per second without cooling. If it is cooled with water flowing in the single channel of 9 mm in diameter at the flow rate of 2 m/s or 7.62 litter/minute (l/m), the temperature will rise by 47.4 K which is too high, but it can be reduced to an N-th of 47.4 K by increasing the number of water channels N. In any way, the cooling water takes all the heat produced on the inner surface of the RF cavity. The bottleneck of the heat transfer is the interface between copper and water. The heat conductivity h from copper to water is given by

$$h = k_{water}\frac{N_u}{d_e} = 9.97\left[\frac{\mathrm{kW}}{\mathrm{m}^2\cdot{}^\circ\mathrm{C}}\right], \quad (1)$$

where k_{water}=0.6245 W/(m K) is the head conductivity of water, Nu=143.7 the Nusselt number given by $Nu = 0.023\times Re^{0.8}\times Pr^{0.4}$ with $Re=2.578\times10^4$ being the Reynolds number and Pr=4.642 the Prandtl number, and d_e=9 mm the effective diameter of the water pipe. This means that the average power is taken from the copper body to cooling water with the temperature difference ΔT = 5.02 K provided that the inner area of the water pipes of 0.5 m^2. This temperature difference sets a certain restriction to the temperature rise of the cooling water. It should be sufficiently lower than twice the temperature difference ΔT so that the heat transfer to cooling water does not vary very much along the cooling water pipes. Assume that the temperature rise of cooling water through the cavity is 2°C, which means that the cooling water system should have 24 parallel water pipes or the flow rate is 183 l/m,

#shigeruk@sanken.osaka-u.ac.jp

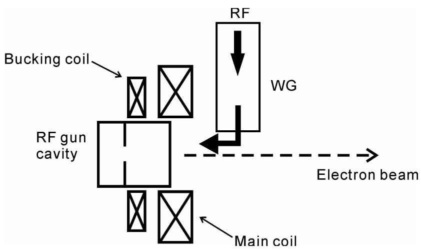

Figure 1: Configuration of RF gun system for simulation.

and that the cavity temperature without the RF input is 50°C, then when the RF power is turned on the input temperature of water is 50°C and the output one should be 52°C. The cavity temperature should be 5°C higher than the mean temperature of cooling water, 51°C, so that it is 56°C or the cavity temperature varies from 50°C to 56°C sometime after the RF power is turned on. This temperature rise of the cavity is close to a limit set by the loaded Q-value of the cavity, ~10^4. In case the temperature rise of cooling water cannot be ignored in comparison with that of the cavity, the temperature of the cavity may not be uniform, resulting in non-uniform deformation of the cavity due to thermal expansion. As a conclusion of these considerations on the static thermal effects, the area of the inner surface of cooling water channels should be as large as possible to reduce the temperature rise of the RF cavity ΔT with the RF input and the flow rate of cooling water should be sufficiently high so that the temperature rise of cooling water in the RF cavity is less than a fraction of ΔT.

Beam Simulation for High Intensity Beam

The parameter scan for the RF gun is performed for two different cases using GPT program [3]. One is the case of ILC specification beam with 3.2 nC bunch charge, another is a high bunch charge case with 30 nC for the SASE experiment at ISIR, Osaka University. The field of the RF gun and solenoid magnet were obtained by SUPERFISH and POISSON code. The simulation was performed with the simplified structure as shown in Fig.1. The cathode surface is set to zero-position in longitudinal direction and the beam properties are calculated at 1.5 m down stream from the cathode. The RF gun cavity assumed the DESY-type L-band cavity, which has 1.5 cells with Cs-Te cahode, and the field of the RF gun cavity is calculated up to 30cm in longitudinal direction. The solenoid magnet for emittance compensation was used the combined type which consists of a main coil, a pure iron yoke and bucking coil as shown in Fig.2 [4]. The solenoid can make a zero magnetic field on the cathode surface to suppress initial emittance growth [5]. The profiles of a laser pulse on the cathode are assumed as Gaussian distribution in longitudinal direction and a uniform radial distribution in transverse direction. Initial transverse emittance is given by $0.64\pi \cdot R$ mm-mrad in the case of a uniform radial distribution with radius R [6].

In the case of ILC specification, the initial beam has 3.2 nC charge, a Gaussian temporal shape with 20 ps length (FWHM) and 3mm radius. The maximum peak filed at the cathode surface of the RF gun is assumed as 41 MV/m which is provided by 3.2 MW rf power. The parameters of the RF gun and solenoids are investigated with the observation at 1.5m point. Figure 3(a) shows the longitudinal properties of the beam, the beam energy and bunch length, as a function of the laser injection phase. Maximum energy gain is 4.7 MeV with 1.7 %(rms) of energy spread. The bunch length increases monotonously with the laser injection phase. Figure 3(b) shows the transverse normalized emittance for three different solenoid strengths. The transverse emittance can be about

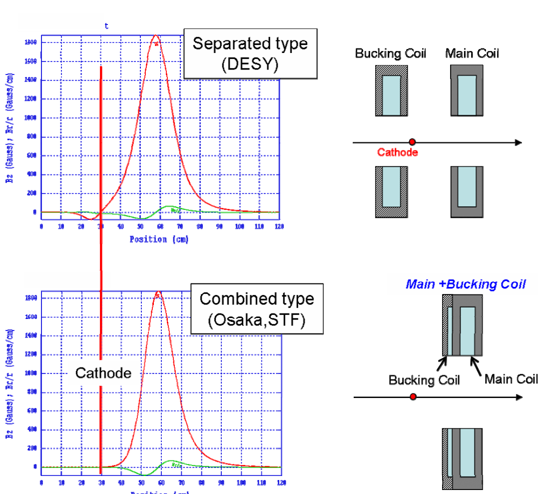

Figure 2: Emittance compensation solenoid of the RF gun. Upper figure shows a separated configuration of bucking and main coils. Lower one is a combined configuration.

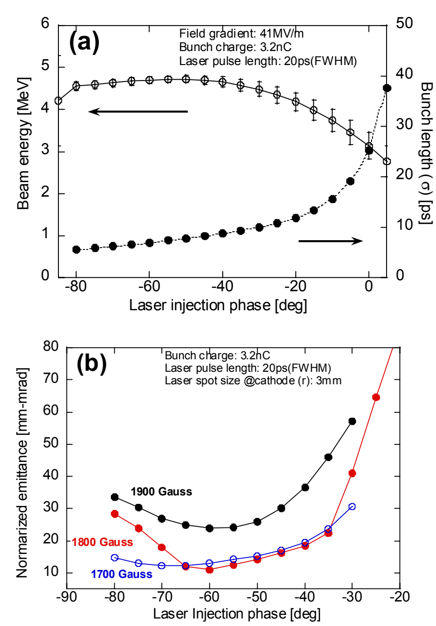

Figure 3: The laser injection phase dependency for beam properties with 3.2 nC bunch charge. (a) Beam energy and bunch length (error bar shows the rms energy spread). (b) Transverse normalized emittance for three different setting of the solenoid.

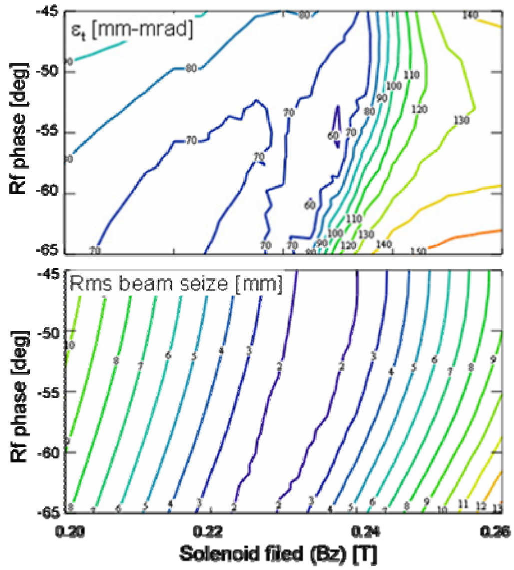

Figure 4: Transverse emittance (top) and rms beam size (bottom) as function of laser launch phase and peak axial magnetic field with 30 nC bunch charge..

10 mm-mrad at -60° of RF phase with 1800 Gauss of solenoid field. By adjusting the solenoid and the laser injection phase, the energy maximum and the transverse minimum can be obtained at the same time.

In the case of SASE experiment at ISIR, the high intensity beam, which has 30 nC charge with ~ 1kA of peak current, passes thorough the wiggler. In the simulation, initial bunch charge is set to 30 nC and the Gaussian temporal shape with 30 ps length (FWHM) and the 7mm radius are assumed to reduce a rapid expansion by space charge around the cathode surface. The maximum peak filed of gun also increases 57.5MV/m to suppress the space charge effects, and the 6.6MW of rf power is required to make this gradient. A drift space after the RF gun and the solenoid field are required for the emittance compensating process. In the optimization to get small transverse emittance, the beam line length from the cathode is assumed as 1.5 m. The backing coil is set to be a zero magnetic field on the cathode. For the parameter scan, the RF phase is varied from -65° to -45° in 2° steps and the peak solenoid field is varied 0.2 T to 0.26 T in 0.004 T steps for 176 simulations. Figure 4 shows that for the parameter scan, the minimum emittance and beam size occur when the RF phase is -56° ~ -54° and the peak magnetic field is 0.234~0.238 T. The emittance of below 70 mm-mrad can be obtained in relatively wide parameter range. (Maximum beam size is limited by the aperture of inner conductor of coupler where beam propagates.)

SASE Radiation Power

SASE output power is calculated using Genesis 1.3 with a high charge and low emittance beam generated the RF gun [7]. The transverse emittance is assumed 70 mm-mrad, which is the result of the above mentioned simulation with 30 nC bunch charge. The electron beam is accelerated to 10 MeV, and it is assumed to be injection to

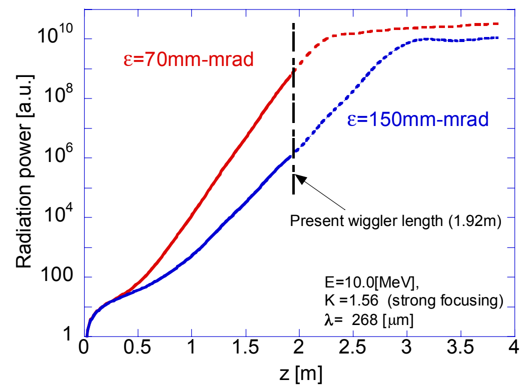

Figure 5: Radiation power as a function of the longitudinal coordinate z for different transverse emittance (70 and 150mm-mrad) with 30nC charge and 30ps bunch length (1.0kA peak current).

wiggler. The wiggler is the strong focusing type that is currently being used in our FEL experiment at ISIR. Focusing and defocusing elements are composed of permanent magnet blocks with the edge angle and they are alternately inserted in magnet arrays of the wiggler [8], and a peak wiggler field of 0.392 T (K = 1.56). Length of real wiggler is 1.92m, but the twice as long wiggler (3.84 m) was assumed for a calculation.

The calculation was performed about two different emittance of electron beam, which are 70 mm-mrad and 150 mm-mrad. Here, the normalized emittance of 150 mm-mrad is typical value that is generated by currently used thermionic electron gun. Figure 5 shows SASE radiation power as a function of the longitudinal coordinate z for different transverse emittance. In this case, the wavelength of SASE is 268 μm. The difference of the saturation power for two cases is only several times, but, as for the radiation power at the position of 1.92m, the case of low emittance is larger almost two orders of magnitude. In the case of present FEL setup at ISIR that the 1.92 m-long wiggler is used, we can get more large SASE power using the low emittance beam generated by RF gun.

RF GUN FOR STF

The main body of the RF cavity for STF-KEK was machined and brazed by FNAL and then it was temporarily sent to KEK for measurement of RF characteristics and frequency tuning. The characteristics of the cavity were measured at a low level with an input coupler made of aluminium for this measurement. The resonance frequency was measured with a network analyzer and the electric field distribution with the bead-perturbation method.

The resonance frequency was measured to be 1301.414 MHz at 25°C, while the target frequency is 1300.00 MHz at the operating temperature of 50°C. The tuning of the cavity has a twofold significance; the frequency tuning and the tuning of the field balance between the half and the full cells. The outer surfaces of end plates of the

Figure 6: Frequency tuning appurtenance of the rf gun cavity.

cylindrical cavity are pressed and deformed with a special tool made for the tuning as shown in Fig. 6. The frequency becomes lower in either case and the electric field becomes lower in a deformed cell, so that the field balance can be varied. In the frequency tuning the temperature difference and the evacuation effect are taken into account. The resonance frequency of the cavity becomes lower due to thermal expansion of copper by 22 kHz/°C with increasing cavity temperature, so that 1300.00 MHz at 50°C is equivalent to 1300.55 MHz at 25°C. When the cavity is evacuated, the frequency becomes 390 kHz higher than that in atmospheric pressure [9] and accordingly the target frequency measured at 25°C in atmospheric pressure is set at 1300.160 MHz. The end plates of the cavity are alternatively and little by little pressed several times with monitoring the resonance frequency of the gun cavity using the dipole or the coaxial coupler. Thus the tuning of the RF cavity is competed, so that the resonance frequency of the π-mode was 1300.187 MHz (0-mode was 1295.140 MHz) and the field balanced is 1.07 as shown in Fig.7. The frequency separation between the π and 0 modes was 5.05 MHz. The unloaded and loaded Q-value of the RF gun cavity are $Q_0 = 23200$ and $Q_L = 9420$ (β=1.46), respectively. The cavity was sent back to FNAL for the final finish to braze cooling water pipes.

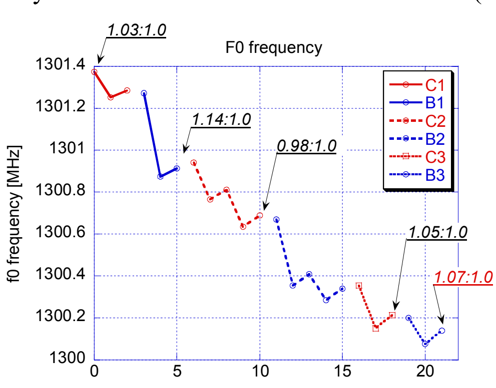

Figure 7: Transition of the resonant frequency and the field balance between the half and full cells of the gun. Red line shows the frequency change when the cathode side is pushed, Blue one shows when the wall of the beam exit side is pushed.

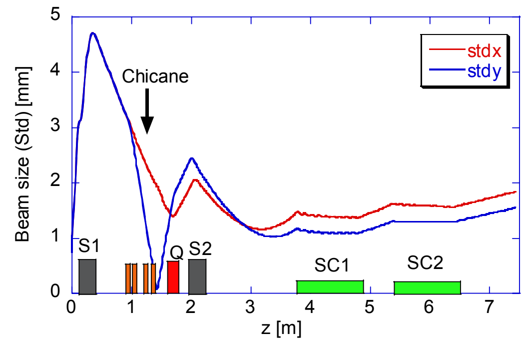

Figure 8: Transverse beam size along the beam line of STF injector section for 3.2 nC bunch charge.

At the KEK-STF, the beam experiment will be performed to demonstrate the multi-bunch (3.2nC x 2820 bunches with 330ns) acceleration of the superconducting rf cavity from the summer of 2010. The L-band RF gun of the DESY type being produced is used as an electron source of the beam experiment. The injector part of STF beam line consists of the L-band photocathode RF gun, the emittance compensation solenoid, a chicane section, a quadrupole magnet, the second solenoid and two 9-cell superconducting accelerating structure. The chicane section, which composed of four rectangular dipole magnets, beam slits, beam monitors, is installed to cut a dark current from RF gun cavity and to measure the beam properties. Figure 8 shows the beam envelope in the STF injector for 3.2 nC bunch charge. The quadrupole is installed downstream of the chicane to control the focusing balance in transverse direction and the second solenoid make the waist at the entrance of first superconducting structure. At the present, the beam line component is produced for the beam experiment in next year.

ACKNOWLEDGMENTS

This study is partly supported by the Supporting Program for Universities in the General Supporting Program on Accelerator Sciences of KEK.

REFERENCES

[1] C. Suzuki et al., Nucl. Instr. Meth. A 462 (2001) 337-348.
[2] H. Matsumoto, Proc. of LINAC96, Geneva, 1996, p.626.
[3] http://www.pulsar.nl/gpt/
[4] B. E. Carlsten, Nucl. Instr. Meth. A285 (1989) 313-319.
[5] D.T. Palmer et al., Proc. of the PAC97 (1997) p2843.
[6] K. Flöttmann et al., TESLA FEL-Report 1997-01, (1997).
[7] http://pbpl.physics.ucla.edu/~reiche/index.html
[8] S. Kashiwagi et al., Proceedings of 27th International FEL Conference (2005) pp199-202.
[9] K. Flöttmann, private communication.